

Effect of Calcination Temperature on ZnO Nanoparticle Crystallinity

Ajay kumar^{1}, Deepak kumar¹, Vikash¹*

^{1*}Associate professor

¹Assistant professor

¹Department of chemistry,

¹Government College for Women, Gurawara, Rewari, 123035, India

^{1*}ajayarjun1980@gmail.com, ¹deepakkumariit56@gmail.com, ¹vikaschahar124@gmail.com

ABSTRACT

Zinc oxide (ZnO) is industrially significant due to properties like corrosion and bacteria resistance, low electron conductivity, and high heat resistance. This study aimed to synthesize ZnO nanostructures using the practical sol-gel method, characterizing them to observe how calcination temperature affects size. The sol-gel method, known for its simplicity and control over morphology, was used to create the nanoparticles from hydrated zinc nitrate and gelatin. The resulting structures were characterized using XRD, FTIR, TGA, and TEM. The synthesized ZnO nanoparticles were found to be homogenous and consistent in size, exhibiting good crystallinity, hexagonal shape, with a size range of 20 nm to 80 nm.

Keywords: ZnO, Nanoparticles, sol gel, Calcination, XRD

I. INTRODUCTION

Metal nanoparticle synthesis is a burgeoning research field attracting significant attention. A variety of synthesis methods have been developed, categorized by phase: vapor-phase techniques (e.g., chemical vapor condensation, arc discharge, laser pyrolysis), liquid-phase methods (e.g., microemulsion, hydrothermal, sol-gel, microbial processes), and solid-phase approaches (e.g., ball milling) [1, 2]. The properties of the resulting nanoparticles are highly dependent on their synthesis procedure.

Metal oxides exhibit a vast range of properties and applications. Zinc Oxide (ZnO) is particularly suitable for sensor and transducer use due to its bio-safe and biocompatible nature. Nanostructured metal oxides possess desirable traits including unique nano-morphological, functional, and catalytic properties [3]. The demand for ZnO nanopowders is growing, driven by their use in industries for ultraviolet filtering, catalysis, anti-corrosion, and anti-bacterial applications. They are commonly used in sunscreens as a UV-resistant additive, and have further applications in electrophotography, capacitors, protective coatings, and conductive thin-films for solar cells and blue laser diodes [4]

Research in nanomaterial synthesis focuses on controlling shape, size, and composition, which dictate material properties and technological uses. Zinc oxide (ZnO), a multifunctional material known for high chemical stability, broad radiation absorption, and photostability, is synthesized via various methods [5, 6]. The specific applications of ZnO nanoparticles rely heavily on control over their physical and chemical properties, including size, shape, surface state, and dispersability [7]. Consequently, numerous synthesis techniques have been developed. Examples include controlled precipitation using zinc acetate and ammonium carbonate by Hong et al. [8], a simple single-step precipitation method by Lanje et al. [9] aimed at cost-effective, large-scale production, and a different controlled precipitation process utilizing NH_4HCO_3 and $\text{ZnSO}_4 \cdot 7\text{H}_2\text{O}$ reported by Wang et al. [10]. Other established methods include the sol-gel technique from zinc acetate dihydrate, oxalic acid, and ethanol by Benhebal et al. [11], and a modified microemulsion approach by Yildirim and Durucan to achieve monodisperse ZnO [12]. In 2014, Kang et al. employed a microfluidic system for the continuous synthesis of zinc oxide nanoparticles for photovoltaic applications [13]. Their study utilized numerical simulations and experimental methods to characterize the ZnO nanoparticles.

II. MATERIAL AND METHOD

MATERIALS

Zinc Nitrate Hydrated ($\text{Zn}(\text{NO}_3)_2 \cdot 6\text{H}_2\text{O}$) was purchased from CDH Fine Chemical (P) Ltd. India. Gelatin powder was purchased from Qualikems Fine Chemicals.

SYNTHESIS OF ZnO NANOPARTICLES

ZnO nanopowder was synthesized using sol gel technique. The glass wares (three necks round bottom flask, measuring cylinder, and beaker) were first cleaned and rinsed with distilled water and dried in oven. All the materials and solvents were weighted with help of electronic weighing balance and mixed in cleaned measuring beaker. 22.5 g of zinc nitrate was dissolved in 50 ml of distilled water and then stirred for 30 min in a cylindrical beaker. Alongside it a 10 g of gelatin was dissolved in 150ml of distilled water and stirred for 30 min at 60 °C to achieve a clear gelatin solution. The temperature was fixed at 80 °C. Stirring was continued for 12 h to obtain a brown resin. The resin became hard after the temperature of the container was reduced to room temperature. The final product was calcined at different temperatures (400, 500, 700 and 900 °C) in air for 8 h to obtain-NPs.

CHARACTERIZATION

X-ray diffraction patterns were determined with a Panalytical's X'Pert powder X-ray diffractometer using $\text{K}\alpha$ radiation ($\lambda=1.5406\text{\AA}$) from a sealed tube operated 30KV and 40 mA. Transmission electron microscopy studies were carried out using a Hitachi H-7500 operated at an accelerating voltage of 80 and 90 KV. The samples for TEM Image were prepared by drop-casting the dispersed particle solution at carbon coated grid.

Thermogravimetric analysis (TGA-DSC); Universal V4.1D TA instruments were used and variation in mass and heat flow was studied in the temperature from ambient to 1,000 °C in a nitrogen atmosphere, at the heating rate of 10°C min⁻¹. FT-IR spectrum of composite sample was taken on the Varian 670-IR spectrometer in the frequency range of 400-4000 cm⁻¹.

III. RESULTS AND DISCUSSIONS

X-RAY DIFFRACTION

Fig. 1a & Fig. 1b shows the XRD patterns of the ZnO-NPs prepared in gelatine media at different calcinations temperatures. All the detectable peaks of the ZnO wurtzite structure without any impurities were observed here. The diffraction pattern is similar to that obtained by Ayudhya et. al.[14]. XRD crystal planes peaks became sharper as the samples were heated at higher temperatures with increasing crystal size.

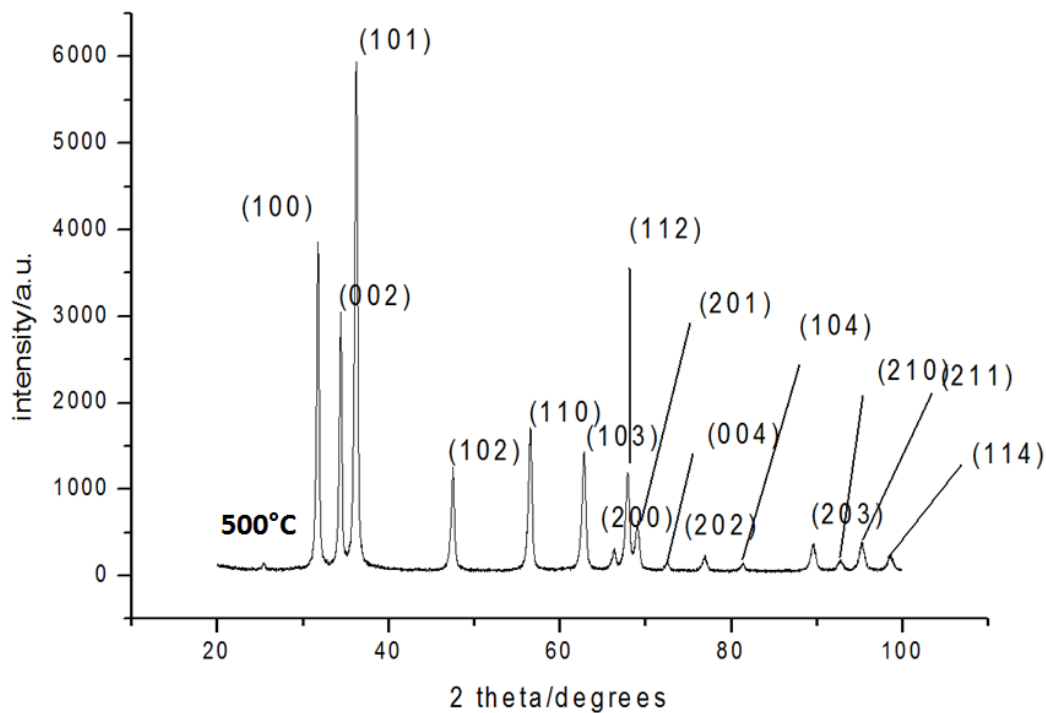


Figure 1a; XRD pattern of ZnO-NPs prepared at different calcination temperatures of 500°C.

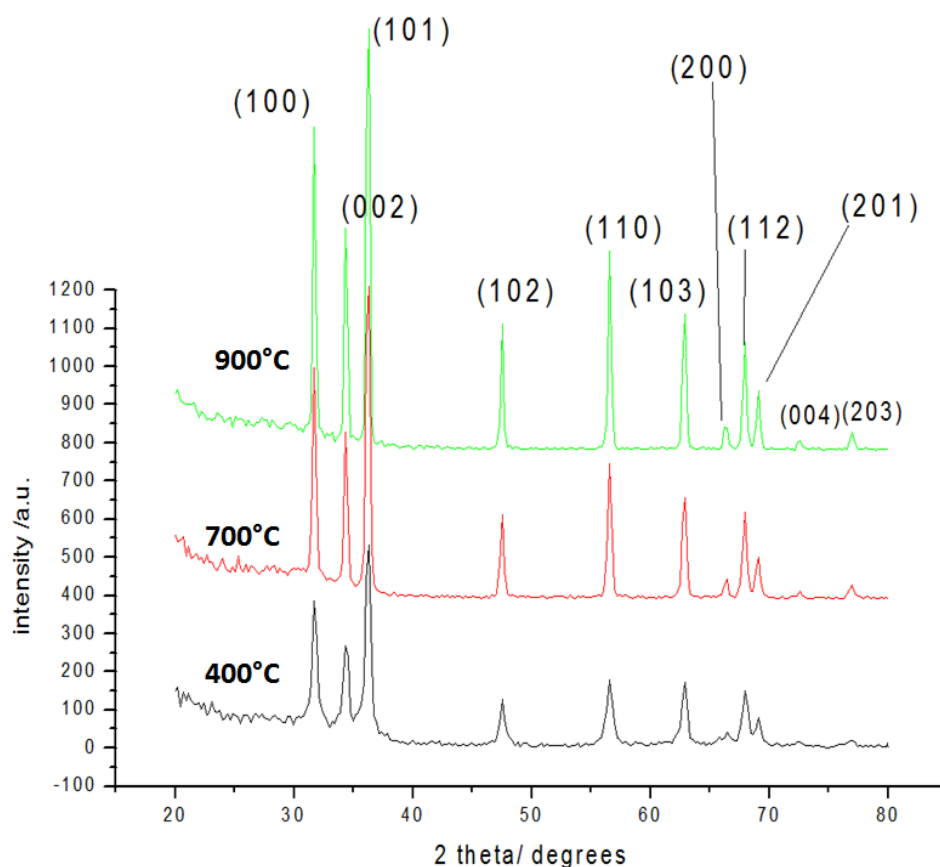


Figure 1b; XRD pattern of ZnO-NPs prepared at different calcination temperatures of 400°C, 700°C, & 900°C.

The wurtzite lattice parameters, e.g., the values of d – the distances between adjacent crystal planes (hkl) – were calculated from the Bragg equation, $\lambda = 2d \sin\theta$. The lattice constants a , b and c ; the interplanar angles, the angle ϕ between the planes ($h_1k_1l_1$) of spacing d_1 and the plane ($h_2k_2l_2$) of spacing d_2 ; and V , the primary cell volumes, were calculated from the Lattice Geometry equation [15]. The (112) and (201) planes can be used to calculate the lattice parameters of the ZnO-NPs calcined at different temperatures.

The crystalline sizes of the ZnO-NPs were determined by means of an X-ray line-broadening method using the Scherrer equation: $D = (k\lambda / \beta \cos\theta)$, where D is the particle size in nanometers, λ is the wavelength of the radiation (1.54056 Å for CuK α radiation), k is a constant equal to 0.94, β is the peak width at half-maximum intensity and θ is the peak position. The (102) plane was chosen to calculate the crystalline size (either plane can be used for this purpose). The crystalline size of the ZnO-NPs calcined at temperatures of 500, 600, and 700 ° and 900C were found are listed below in the Table 1.

Table 1: Crystalline Size of ZnO nps. Calcined at various temperature

	Sample	Crystalline Size
a)	ZnO@500°C	30 nm
b)	ZnO@600°C	50 nm
c)	ZnO@700°C	70 nm
d)	ZnO@900°C	90 nm

FTIR SPECTROSCOPY

FTIR as used to identify the functional groups and identification quality finished products. FTIR was performed Spectrum RX-I with a resolution of 1 cm^{-1} and scan range of 4000 cm^{-1} to 250 cm^{-1} . Fig. 2 shows the FTIR spectra of the ZnO samples calcined at different temperatures.

Table 2: Characteristic absorption bands of Calcined ZnO nps

	ZnO @ 500	ZnO @ 700	ZnO @ 900
O–H stretching	3380 cm^{-1}	3408 cm^{-1}	3406 cm^{-1}
Carboxylate And Hydroxyl impurities	1449 cm^{-1} , 1161 cm^{-1} 1125 cm^{-1}	1447 cm^{-1} 1171 cm^{-1} 1110 cm^{-1}	1456 cm^{-1} 1110 cm^{-1} 1158 cm^{-1}
ZnO	400 cm^{-1}	400 cm^{-1}	400 cm^{-1}

For the FTIR spectra of the calcined samples at 400, 500, 700 and 900 °C, a series of absorption peaks from 1000 to 4000 cm^{-1} can be found, which correspond to the carboxylate and hydroxyl impurities in the materials although the level of impurities decreased as the calcination temperature increased. More specifically, the broad band at 3420 cm^{-1} was assigned to the O–H stretching mode of the hydroxyl group. The peaks observed at 1449, 1161, 1125 cm^{-1} are due to the asymmetrical and symmetrical stretching of the zinc carboxylate in case of ZnO synthesized at 500°C [16]. Characteristic absorption bands are shown in Table 2. As shown in the FTIR traces, the spectral signatures of carboxylate impurities disappear as the calcination temperature increases. This indicates the possibility of zinc carboxylate dissociation and conversion to ZnO during the calcination process. For all of the samples in this study, a broad absorption band was observed at around 400 cm^{-1} . The band at around 400 cm^{-1} corresponds to the absorption spectra of hexagonal ZnO [17].

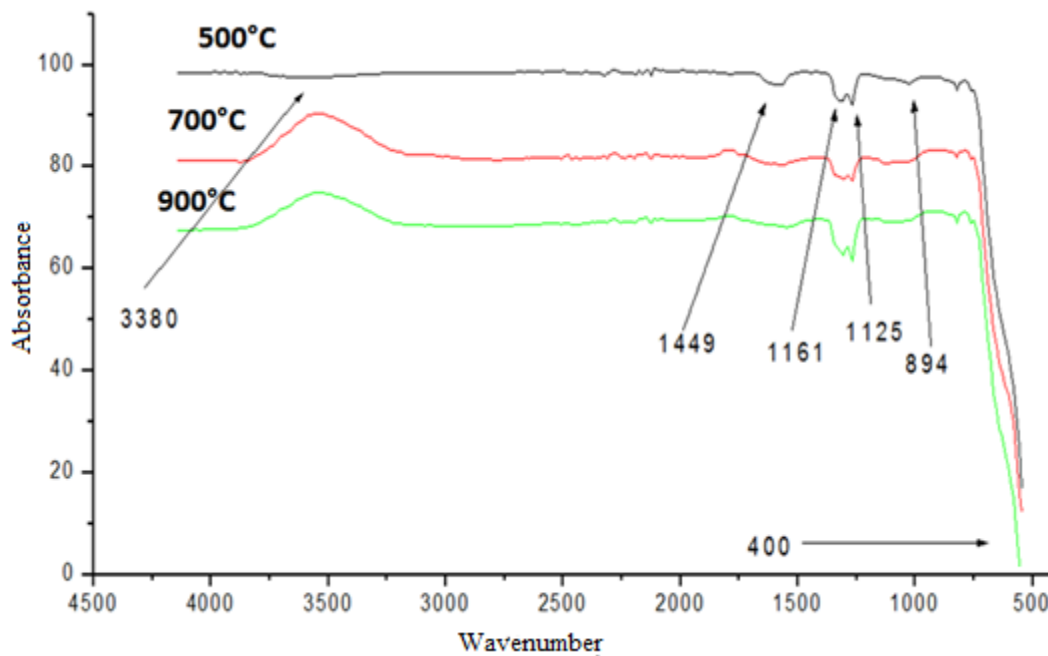


Figure 2: shows the FTIR spectra of the ZnO samples

THERMO GRAVIMETRIC ANALYSIS

Thermo gravimetric analysis or thermal gravimetric analysis (TGA) is a method of thermal analysis in which changes in physical and chemical properties of materials are measured as a function of increasing temperature (with constant heating rate), or as a function of time (with constant temperature and/or constant mass loss).

The thermo gravimetric and derivative analyze (TGA/DTA) curves of the ZnO-NPs presented in Fig. 3. The TG curve descends until it becomes horizontal around 550 °C. The TG and DTA traces show three main regions. The first weight loss between 50 and 170 °C (27.61%) is an initial loss of water—bend Ed1. The second weight loss from 170 to 295 °C (25.73%) is attributed to the decomposition of chemically bound groups, which corresponds to bend Ed2. The third step from 220 to 550 °C (18%) is related to both the decomposition of the organic groups and the formation of the pyrochlore phases and to the decomposition of the pyrochlore phases and the formation of ZnO pure phases—bend Ed4. No weight loss between 500 and 600 °C was detected on the TG curve, which indicates the formation of nanocrystalline ZnO as the decomposition product. TGA results showed the phase transforming mechanism of the calcinations process which showed that at around 550°C temperature TGA curve becomes constant which showed that at that temperature no more quantity of gelatin is left and the decomposition temperature of zinc nitrate is between 130°C-150°C i.e. at that temperature ZnO starts forming and the entire phase transformation takes place at around 500°C.

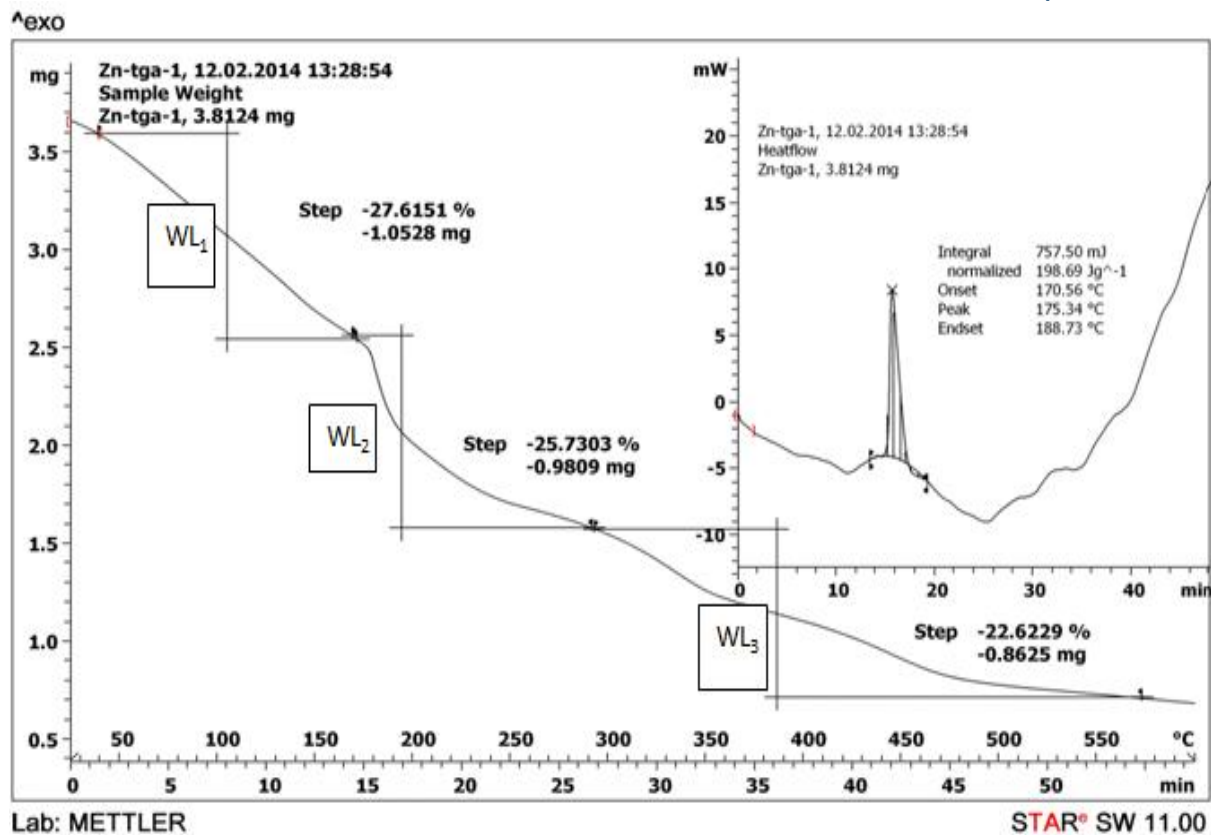


Figure.3: TGA and DTA curves of gels from 50 °C to 600 °C.

TRANSMISSION ELECTRON MICROSCOPY (TEM)

The morphology and size distribution of the ZnO-NPs calcined at temperatures of 500, 700, and 900 °C are shown in Fig. 4, Fig. 5, Fig. 6.

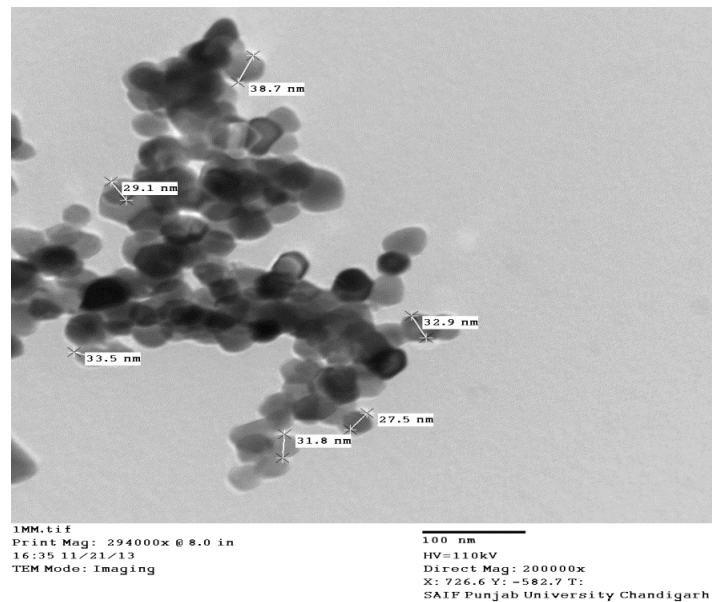


Figure 4: TEM images of ZnO-NPs prepared @ 500°C

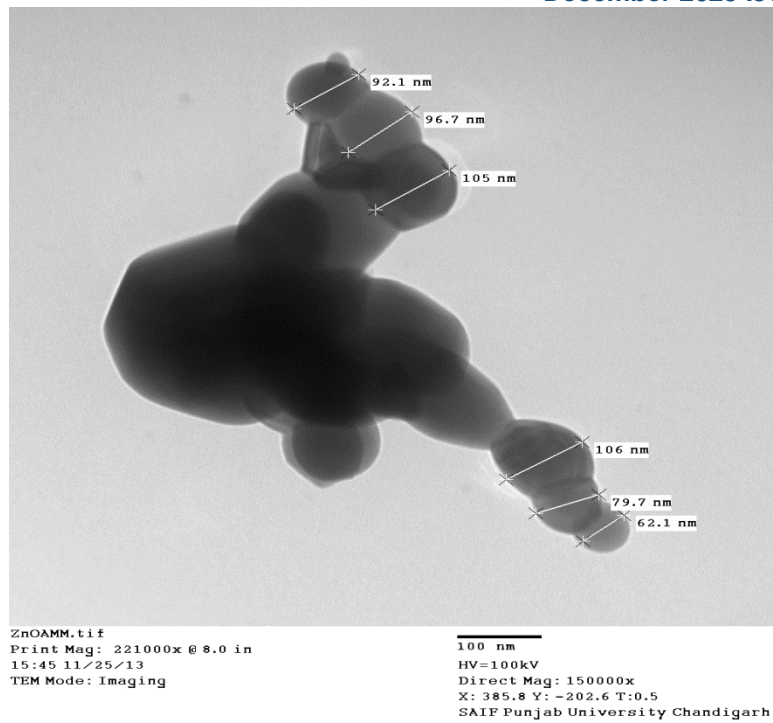


Figure 5: TEM images of ZnO-NPs prepared @ 700°C

It can be clearly observed that the nanoparticles grew as the calcinations temperature increased it is because as the temperature is increased the capping agents decreases and they simply burn off which results in aggregation of ZnO particles of higher size. It was also observed that both hexagonal and circular shapes were exhibited by the nanoparticles that were calcined at 500°C however there it was observed the aggregated and overlapped structures that can might be because of lack of dispersion due insoluble nature of ZnO nanoparticle . The number of hexagonally shaped nanoparticles increased as the calcinations temperature increased, or said another way, the growing size increased the number of hexagonally shaped nanoparticles. This event can be related to quantum size effects. When the size of the particle is very small, the ratio of the atoms on the surface to all of the atoms in the particle increases. In this situation, the surface atoms can affect the morphology of the particle [18]. When the size of the particles grows, the ratio of the atoms on the surface to all of the atoms in the particle decreases. At a certain point, the effect of the surface atoms is negligible. The size histograms of the ZnO-NPs are shown below the relative TEM images. The TEM results showed that the main particle size of the ZnO-NPs calcined at temperatures of 500, 700, and 900 °C were about 29 ± 5 , 40 ± 10 , and 58 ± 15 nm, respectively. The TEM and size distribution results confirm that a narrow size distribution can be obtained for ZnO-NPs prepared with gelatin media and calcined at temperatures of 500, 600, and 700 °C.

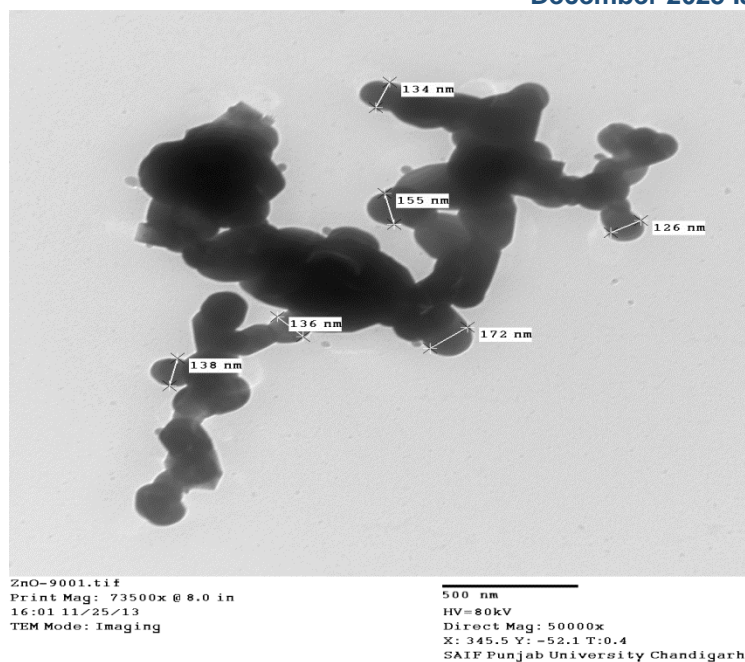


Figure 6: TEM images of ZnO-NPs prepared @ 900°C

IV. CONCLUSION

ZnO nanoparticles were synthesized by the sol-gel method in gelatin media. This method used was comparatively quite simple to understand, low cost and had a large scale industrial output, which showed its potential for industrial application. Further from XRD pattern it was observed that the ZnO nanoparticle had a highly crystalline structure and the crystallinity of the nanoparticle increased with the increase in the calcination temperature, which was observed with much sharper peaks in XRD diffraction patterns. Also, the crystalline size of the nanoparticle was calculated using the Scherrer equation, and the crystal size increased with the increase in temperature. Average crystalline size of ZnO nanoparticles calcined at different temperatures of 500°C, 600°C, 700°C and 900°C are 30 nm, 50 nm, 70 nm, 90 nm respectively. From FTIR it was observed that there were relatively very few impurities; it can be observed that all of the ZnO-NPs calcined at different temperatures exhibited the hexagonal, wurtzite structure. TGA results showed the phase transforming mechanism of the calcination process, which showed that at around 550°C temperature the TGA curve becomes constant, which showed that at that temperature no more quantity of gelatin is left and the decomposition temperature of zinc nitrate is between 130°C-150°C i.e. at that temperature ZnO starts forming and the entire phase transformation takes place at around 500°C. On increasing the calcination temperature, the crystallinity improved. Gelatin used in the reaction acts as a good stabilizer and polymerization agent to prepare ZnO-NPs on a large scale using the sol-gel method.

V. ACKNOWLEDGEMENT: The authors are gratefully acknowledge to Dr. Vishal Sharma and Dr. Neeraj Kumar from chemistry department of Panjab University, Chandigarh, Haryana, India for providing all support during the study period

VI. CONFLICT OF INTEREST: The authors have no conflict of Interest.

REFERENCES:

1. Kargari, A. Tavakoli, M. Sohrabi. A review of methods for synthesis of nanostructured metals with emphasis on iron compounds. *Chemical Papers*, 2007, 61 (3), pp. 151–170.
2. Research and market. The Global Market for Metal Oxide Nanoparticles to 2020. *Research and Markets*, 2013. Retrieved from http://www.researchandmarkets.com/reports/2488811/the_global_market_for_metal_oxide_nanoparticles.
3. Wahab, H.A., Salama, A.A., et al. Optical, structural and morphological studies of ZnO nano-rod thin film using sol-gel. *Journal Name Not Provided*, 2013, 3, pp. 46–51.
4. Chai, C. The Global Market for Zinc Oxide Nanopowders 2012. *New Report on Global Zinc Oxide Nanopowder Market*, 2012, pp. 135–140.
5. Segets, D., Gradl, J., Taylor, R.K., Vassilev, V., Peukert, W. Analysis of optical absorbance spectra for the determination of ZnO nanoparticle size distribution, solubility, and surface energy. *ACS Nano*, 2009, 3, pp. 1703–1710.
6. Guo, R., Lou, X.J. Synthesis of ZnO Nanoparticles by precipitation method. *Sens. Trans. Technol.*, 1991, 3, pp. 1–5.
7. Wahab, R., Ansari, S.G., Kim, Y.S., Seo, H.K., Shin, H.S. Room temperature synthesis of needle-shaped ZnO nanorods via sonochemical method. *Appl. Surf. Sci.*, 2007, 253, pp. 7622–7626.
8. Hong, R., Pan, T., Qian, J., Li, H. Synthesis and Surface Modification of ZnO Nanoparticles. *Chem. Eng. J.*, 2006, 119, pp. 71–81.
9. Lanje, A.S., Sharma, S.J., Ningthoujam, R.S., Ahn, J.S., Pode, R.B. Low temperature dielectric studies of zinc oxide (ZnO) nanoparticles prepared by precipitation method. *Adv. Powder Technol.*, 2013, 24, pp. 331–335.
10. Wang, Y., Zhang, C., Bi, S., Luo, G. Preparation of ZnO nanoparticles using the direct precipitation method in a membrane dispersion micro-structured reactor. *Powder Technol.*, 2010, 202, pp. 130–136.
11. Benhebal, H., Chaib, M., Salomon, T., Geens, J., Leonard, A., Lambert, S.D., Crine, M., Heinrichs, B. Alex. Photocatalytic degradation of phenol and benzoic acid using zinc oxide powders prepared by sol-gel process. *Eng. J.*, 2013, 52, pp. 517–523.
12. Yildirim, O.A., Durucan, C. Synthesis of zinc oxide nanoparticles elaborated by microemulsion method *J. Alloy. Compd.* 2010, 506, pp. 944–949.
13. Kang, H.K.; Leem, J.; Yoon, S.Y.; Sung, H.J. Continuous synthesis of zinc oxide nanoparticles in a microfluidic system for photovoltaic application. *Nanoscale*. 2014, 6, 2840–2846.

14. Ayudhya, S.K.N.; Tonto, P.; Mekasuwandumrong, O.; Pavarajarn, V.; Praserttham, P. Solvothermal Synthesis of ZnO with Various Aspect Ratios Using Organic Solvents. *Cryst. Growth Des.* **2006**, 6, 2446.
15. Cullity, B.D. *Elements of X-ray diffraction: a practical approach*; Addison-Wesley Publishing Company Inc.: California, 1956.
16. Xiong, G.; Pal, U.; Serrano, J.G.; Ucer, K.B.; Williams, R.T. Photoluminescence and FTIR study of ZnO nanoparticles: the impurity and defect perspective. *Phys. Status Solidi C* **2006**, 3, 3577–3581.
17. Roselli, M.; Finamore, A.; Garaguso, I.; Britti, M.S.; Mengheri, E. Antimicrobial activities of commercial nanoparticles against an environmental soil microbe, *Pseudomonas putida* KT2440. *J. Nutr.* **2003**, 133, 4077–4082.
18. Hosokawa, M.; Nogi, K.; Naito, M.; Yokoyama, T. Nanoparticle Technology handbook, Elsevier: Amsterdam, 2007.